JOURNAL OF PROPULSION AND POWER
Vol. 13, No. 5, September–October 1997

Performance Limits for Projectile Flight in the Ram and External Propulsion Accelerators

J. Rom*
Technion—Israel Institute of Technology, Haifa 32000, Israel

There is a great advantage in developing accelerators of projectiles using chemical propellants because the chemical propellants are about three orders of magnitude more compact in weight and size than electromagnetic energy storage systems. The in-tube chemical accelerator methods are the experimentally proven ram accelerator (RA) and the proposed external propulsion accelerator (EPA). The total thrust generated on the projectiles in these chemical accelerators is obtained from the energy released in the chemical reactions. The net thrust for accelerating the projectile is obtained from the difference between the total thrust and the total drag of the flying projectile. The experiments in the RA, where the titanium-nosed projectile exited the tube intact, are used to validate this energy balance method. In these tests the instantaneous acceleration as well as the maximum terminal velocity of the projectile in the RA are measured. These measurements are used to evaluate the drag coefficient of the flying projectile and the propulsive efficiency. The experimental data of tests in the RA at the University of Washington show that as the projectile approaches its maximum terminal velocity, the evaluated drag coefficient reaches values of about 1.5, while the evaluated propulsive efficiency is about 0.8. Then, the maximum projectile terminal velocity in the RA calculated by the energy balance method is about 1.2 times the detonation velocity. Then, the maximum projectile velocity in the RA (which is up to 1.2 times the detonation velocity), for mixtures of detonation velocity up to 2.5 km/s, will be about 3 km/s. The energy balance analysis shows that the corresponding maximum terminal velocity of a free-flying aerodynamically stabilized projectile in the EPA can reach up to about six times the Chapman–Jouguet detonation velocity. The energy balance analysis indicates that the EPA can be used to accelerate a free-flight projectile to velocities of well beyond escape velocity. This EPA system has the potential to be considered for the development of a one-stage-to-orbit launcher.

Nomenclature

a = acceleration
C_D = drag coefficient
D = drag
D_{CJ} = Chapman–Jouguet detonation velocity
d = body diameter
H = step height
h = altitude
M = Mach number
p = pressure
Q = chemical energy per unit mass
S = projectile reference area
T = thrust
T_∞ = undisturbed flow temperature
V = projectile velocity
W = weight
β = ratio of combustion region diameter to projectile diameter
γ = specific heats ratio
η_p = propulsive efficiency
λ = detonation cell size
ρ = density

Introduction

THE development of in-tube chemical accelerators is motivated by the fact that the chemical propellants are about three orders of magnitude more compact in weight and size than electromagnetic energy production and storage systems (Table 1). Therefore, there is a great advantage in developing accelerators of projectiles using chemical propellants. There are two methods for in-tube chemical accelerators utilizing premixed gaseous detonative mixtures: 1) the experimentally proven ram accelerator (RA) and 2) the proposed external propulsion accelerator (EPA). These in-tube chemical launchers for accelerating projectiles to hypervelocity utilize, in the superdetonative mode of operation, the possibilities of generating continuous thrust by initiating combustion–detonation in the premixed fuel/oxidizer mixture by shock-wave interactions. Recent developments in the research on the EPA are presented in Refs. 1 and 2.

The first method proposed for an in-tube chemical launcher was the RA (developed by Hertzberg et al.).[3] The concept of the RA, operating in the superdetonative mode, is based on utilization of the scramjet cycle, where the projectile acts as a free centerbody and the tube as an extended cowling (Fig. 1). The sharp-nosed projectile diameter is slightly less than the tube diameter (typically 70–80%). Therefore, the nose shock wave is reflected from the tube wall into the projectile centerbody. Under proper conditions this reflected shock wave initiates a combustion–detonation process so that when the products of the chemical reactions are expanded on the rear part of the projectile, thrust is generated. The projectile is centered in the launching tube by four, five, or six fins attached to the projectile. These fins span the short distance from the projectile body to the tube wall.

It is important to note that in the RA the shock-wave reflections from the tube wall are the mechanisms for inducing the combustion–detonation on the projectile in the superdetonative mode of operation. There is a strong interaction between the supersonic flow in the narrow passage (between the projectile and the tube wall) with the reflected shock–detonation waves inducing the heat release by the chemical reac-

Received Feb. 2, 1996; revision received Aug. 1, 1996; accepted for publication March 29, 1997.

*Professor, Lady Davis Chair, Faculty of Aerospace Engineering, part of this work was done while the author was a Visiting Professor, Department of Aerospace Engineering, University of Maryland, College Park, MD 20742. Fellow AIAA.

Table 1 Comparison of energy storage volume and weight for chemical and electromagnetic systems

Materials	Mass, 1 MJ (discharge time)	Energy density, MJ/m^3
Detonative gases	0.1 kg (μs)	$0.1-2.6 \times 10^3$ @ 100 atm
Explosives	0.2 kg (μs)	8.0×10^3
Propellants	0.35 (ms)	4.6×10^3
Battery	5.0 kg (h)	——
	5.0 ton (ms)	0.55
Flywheel	100 kg @ 10^4 rpm (ms)	——
Capacitors	6.0 ton (μs)	0.06–0.6
Inductors	0.2 ton (ms)	45

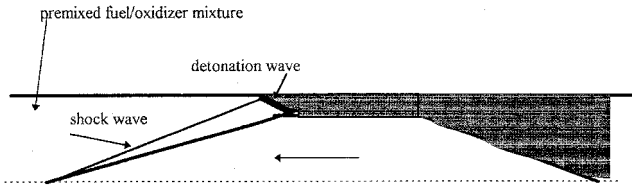

Fig. 1 RA projectile in superdetonative mode.

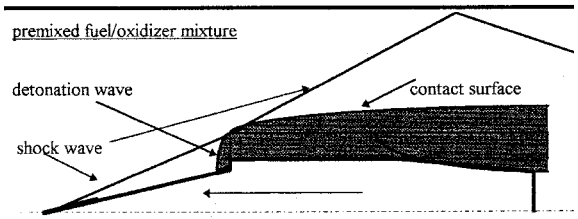

Fig. 2 EPA projectile with a forward-facing step.

tions. The deposition of the large heating rates into the supersonic flow in the narrow passage may lead, under certain conditions, to thermal choking. This may be one of the mechanisms causing the unstart in the RA operations.

Another method for operating the chemical in-tube accelerator is based on the utilization of the external propulsion cycle.[4] In the EPA it is proposed to fire the projectile into the launcher tube that is filled with the premixed fuel/oxidizer mixture. However, here the projectile diameter is only about 25–40% of the tube diameter. For this subcaliber projectile there is no interaction with the tube wall over the complete length of the projectile (Fig. 2). The combustion–detonation is initiated and confined to the rear part of the projectile only by aerodynamic means. A forward-facing step or ramp on the projectile shoulder or a blunt leading edge of a ring wing positioned on the center/rear part of the projectile are used for initiating combustion–detonation. By the interactions of the detonation wave with the nose shock wave an external combustion chamber is produced. This external combustion region is confined by the contact layer generated at the intersection point between the nose shock wave and the detached detonation wave ahead of the step. The contact layer separates the high-temperature reaction products from the outer layer of nonreacting flow. The pressure imposed on the contact region is determined by the pressure jump behind the transmitted oblique shock–detonation wave. This pressure is higher than the freestream pressure and is increased as the flow Mach number increases. Thus, the aerodynamically confined combustion region is filled with the hot chemical reaction products compressed to higher pressure by the transmitted shock wave. The hot compressed combustion products are then expanded on the rear part and into the base region of the projectile, producing thrust on the projectile. The projectile flies freely (including the possibility of rolling rotation) in the launch tube and is stabilized aerodynamically by fins to maintain its trajectory about the tube centerline. Some analytical and numerical calculations of the characteristics of the EPA and various applications are discussed in Refs. 5–9. The computational fluid dynamics (CFD) calculations indicate that it is possible to establish and stabilize a combustion–detonation front on projectiles flying at hypersonic speeds in detonable gas mixtures. The establishment of a combustion front ahead of the forward-facing step and on spherical-nosed blunt bodies in hypersonic flows of detonable mixtures were analyzed.[10–12] The flow established on a 15-deg half-angle cone with a 45-deg ramp fired at Mach 5 into a hydrogen–air mixture was photographed by Lehr.[13] The interaction between the nose shock wave and the detonation–combustion front established ahead of the blunt ramp is clearly seen, including the generation of the contact layer from the intersection point. This flow structure validates the flow model used in the EPA analysis and calculations.

There are expected difficulties in obtaining sufficient aerodynamic stability and clean sabot separation to ensure the free-flight trajectory of the projectile in the EPA. Therefore, the present study includes the possibility of using fin-guided projectiles in the EPA. It may be advantageous to begin EPA operations by incorporating mechanical guides for centering the projectile in the launching tube of the EPA. The projectile can be centered by wide-span fins attached to the subcaliber projectile body extending to the tube wall (fin guided). Instead of the wide fins, the projectile can be centered by rails built into the tube walls (rail guided). This arrangement is similar to the rail guides in the RA discussed in Ref. 14, except that in the EPA application the span of the rails must be much wider. The versions of the fin-guided and rail-guided projectiles in the EPA are new applications for the in-tube chemical accelerators. The body diameter of the subcaliber projectile, for this application, can be in the range of 25–45% of the launcher tube diameter (different from the 70% in the RA case). In this case the fin-guided EPA projectile is centered in the launching tube similarly to the fin guiding in the RA. However, it should be noted that in the EPA case, the combustion is induced by a small step or ramp on the subcaliber projectile body. Using the subcaliber projectile in the fin-guided EPA eliminates the interaction with the tube wall and the large drag rise experienced at high Mach numbers in the RA.

This paper presents the analysis of the projectile flight performance using the energy method. This energy method is derived from the energy-state method used in aircraft performance. Relevant experimental results of tests in the RA are reviewed and their results are used to validate the analysis. The analysis can be applied to the evaluation of limits of the performance of projectile flight in the RA, in the free-flight EPA, and for the fin-guided projectiles in the EPA. The application of the energy balance analysis to evaluate the maximum velocity of projectiles that can be achieved in the RA was discussed by Lee.[15] This analysis was applied to the evaluation of the velocity of projectiles in the RA and EPA.[16,17]

Energy Method for Analysis of Projectile Flight Performance in the In-Tube Chemical Accelerator

For modern aircraft, having high-thrust and high-acceleration capabilities, it is advantageous to use the energy-state analysis for performance calculations. This energy-state

method is based on the definition of the total energy that is the sum of the potential energy and the kinetic energy of the accelerating aircraft. Then, using the force balance on the accelerating aircraft, it is shown that the performance equation (e.g., Ref. 18), is as follows:

$$\frac{dh}{dt} = \frac{V(T - D)}{W} - \frac{V}{g}\left(\frac{dV}{dt}\right) \tag{1}$$

In level flight, $dh/dt = 0$, corresponding to the flight of the projectile in the launching tube of the chemical accelerator, therefore, the equation for the acceleration of the projectile is

$$\left(\frac{dV}{dt}\right)\Big/ g = \frac{a}{g} = \frac{T - D}{W} \tag{2}$$

The projectile reaches its maximum velocity when $a/g = 0$, when thrust = drag. T is obtained from the conversion of the energy released in the chemical reaction in the hypersonic flow over the projectile to forward axial force. D is the total aerodynamic drag including the effects of combustion on the drag of the projectile. In addition, the drag caused by friction, in the cases of fin or rail-guided projectiles, should be included.

Evaluation of the Thrust Acting on the Projectile in the In-Tube Chemical Accelerators

The thrust force acting on the projectile can be evaluated by integrating the pressure distribution acting on its surfaces. It can also be evaluated by the momentum balance across a control surface surrounding the projectile. Both of these methods require the calculation of the flow characteristics over the projectile. Another method for evaluation of the thrust is by estimating the part of the total energy released by the chemical reactions that is converted to thrust force by defining η_p. The chemical kinetics and thermodynamics of the propulsion are incorporated into the integrated definition of η_p. The mass flow rate of the combustible mixture into the reaction region on the projectile is the following:

$$\rho_\infty \left[\frac{\pi(\beta d)^2}{4}\right] V_\infty$$

This mass flow rate is then multiplied by the heat energy released per kilogram of mixture gives the rate of total energy released. When the mass flow rate is multiplied by η_p, it gives the rate of thrust energy, which is equal to TV_∞:

$$\rho_\infty \left[\frac{\pi(\beta d)^2}{4}\right] Q V_\infty \eta_p = TV_\infty \tag{3}$$

The propulsive efficiency must be evaluated by theoretical or empirical considerations. It will be shown that the propulsive efficiency for the projectile in the RA can be evaluated by utilizing the measurements of projectile acceleration in the RA. The propulsive efficiency can be expressed by the relation, using Eq. (3):

$$\eta_p = \frac{4TV_\infty}{Q\rho_0 V_\infty \beta^2 \pi d^2} \tag{4}$$

Thus, the propulsive efficiency represents the ratio of the rates of the thrust energy to the total available chemical reaction energy. The relation for the propulsive efficiency [Eq. (4)], can be expressed in terms of the thrust parameter $T/p_\infty S$ and the heat addition parameter Q/c_pT_∞:

$$\eta_p = \frac{\gamma - 1}{\gamma}\frac{(T/p_\infty S)}{(Q/c_pT_\infty)\beta^2} \tag{5}$$

Performance estimates of the RA and EPA (Refs. 1–3) indicate that thrust parameter values $T/p_\infty S$ of about 2–6 can be achieved. The heat addition parameter Q/c_pT_∞ in the mixtures proposed for the chemical accelerators have values of about 2.5–8 and γ values of about 1.3–1.4. In the RA the $\beta = d_{\text{tube}}/d_{\text{projectile}}$ value is about 1.3, whereas for the EPA operation β values of about 1.2–4 are anticipated. In these cases the values of the propulsive efficiency, evaluated by Eq. (5), extend to between 0.1–0.8. This large range of values indicates that careful evaluation of each of the parameters is required to obtain reasonable estimates for the performance of the projectile in the in-tube chemical accelerators.

Evaluation of the Drag Acting on the Projectile in the In-Tube Chemical Accelerators

Drag on the Projectile in the Ram Accelerator

The total drag acting on the projectile flying in the RA includes 1) the aerodynamic drag of the free-flying projectile, 2) the drag caused by the friction of the fins sliding on the tube wall, and 3) the drag caused by the stagnation pressure loss in the supersonic flow with heat addition in the narrow passage between the shoulder of the projectile and the tube wall. The total pressure loss is because of the heat added to the supersonic flow by the chemical reactions induced by the reflected oblique shock waves. These reflected shock waves, from the tube wall into the projectile body, initiate the exothermic chemical reactions in this zone. The characteristics of the supersonic flow in a channel with a variable cross-sectional area and with heat addition are discussed in Ref. 19. These effects of heat addition and area change on the flow characteristics are presented as follows:

$$\frac{du}{u} = \frac{1}{1 - M^2}\frac{dQ}{c_pT} - \frac{1}{1 - M^2}\frac{dA}{A}$$

$$\frac{d\rho}{\rho} = -\frac{1}{1 - M^2}\frac{dQ}{c_pT} + \frac{M^2}{1 - M^2}\frac{dA}{A}$$

$$\frac{dp}{p} = -\frac{\gamma M^2}{1 - M^2}\frac{dQ}{c_pT} + \frac{\gamma M^2}{1 - M^2}\frac{dA}{A}$$

$$\frac{dT}{T} = \frac{1 - \gamma M^2}{1 - M^2}\frac{dQ}{c_pT} + \frac{(\gamma - 1)M^2}{1 - M^2}\frac{dA}{A}$$

$$\frac{dM}{M} = \frac{1 + \gamma M^2}{2(1 - M^2)}\frac{dQ}{c_pT} - \frac{2 + (\gamma - 1)M^2}{2(1 - M^2)}\frac{dA}{A}$$

$$\frac{dP_t}{P_t} = \frac{\gamma M^2}{2 + (\gamma - 1)M^2}\frac{dQ}{c_pT}$$

The condition for choking is

$$\left(\frac{Q}{c_pT}\right)_{\max} = \frac{(1 - M^2)^2}{2(\gamma + 1)M^2}$$

The total pressure loss is increased with higher heat addition and with increasing Mach number. High heat addition, above the value allowed for the flight Mach number, may cause choking of the supersonic flow. The condition for choking is also indicated earlier. The normal shock wave established in the case of choking of the flow results in a very large drag. This high drag slows down the projectile so that the combustion may jump upstream of the nose of the projectile, leading to the unstart. Thus, the total drag must include the drag caused by the total pressure loss because of heat addition in the supersonic flow in the narrow passage. This total drag can be evaluated using the present energy balance analysis from some of the experimental results obtained in the RA. The method of evaluation of the total drag coefficient of the projectile using the data obtained in RA tests is discussed later in this paper.

Drag on the Projectile in the External Propulsion Accelerator

The flow over the projectile in the EPA is independent from interactions with the tube wall. The subcaliber projectile is assumed to fly freely in an atmosphere of the combustible mixture inside the tube. Therefore, the aerodynamic characteristics of the projectile can be estimated and/or measured by well-known aerodynamic methods. The drag coefficient of a representative projectile geometry, shown in Fig. 3, is measured in the supersonic wind tunnel in the Aerodynamic Laboratory at Technion. The forward part of the projectile has a 10-deg half-angle conical nose and a 1-mm blunt step followed by a 32-mm cylindrical section. The back part is composed of a shallow boattail aftbody with fins and a blunt base (Fig. 3). For reference a model with a similar conical nose but without a step is also tested. The drag coefficient's variation as a function of angle of attack, for both the clean cone and the cone and step models, is measured at Mach numbers 2.5 and 3.4. Re_D in these wind-tunnel tests is about 1.4×10^6. This Reynolds number is much lower than the expected Reynolds number in the EPA, which is in the order of 10^8. Therefore, the drag caused by the step in the wind-tunnel test is probably reduced because of the boundary-layer separation ahead of the forward-facing step. At the lower Reynolds number a shallow ramp-type separation is established ahead of the forward-facing step. At the high Reynolds number, expected in the EPA, the boundary layer is much thinner and the ramp separated zone ahead of the step is expected to be much more blunt. Therefore, a reasonable conservative estimate of the drag caused by the step on the projectile in the EPA is to equate it to that of a blunt body with $C_D = 1$. The contribution of the drag of the step to the total drag of the projectile is weighted by the area ratios of the step-forward area to the projectile cross-sectional reference area. In this case the drag coefficient for the projectile with a step in the EPA is evaluated by

$$C_D = C_{D_{\text{projectile}}} + C_{D_{\text{step}}}(S_{\text{step}}/S_{\text{projectile}}) \tag{6}$$

where S_{step} is the frontal area of the step, and $S_{\text{step}} = \pi\, \mathrm{d}H$ and $S_{\text{projectile}}$ is the maximum cross-sectional area of the projectile $S_{\text{projectile}} = \pi d^2/4$. The drag coefficient of the projectile $C_{D_{\text{projectile}}}$ is equal to the drag coefficient of the clean conical projectile without the step. The relation for the total drag of the projectile with the step becomes

$$C_D = C_{D_{\text{projectile}}} + (4H/d)C_{D_{\text{step}}} \tag{7}$$

The drag coefficient of the cone–cylinder–boattail free-flight projectile with fins (without a step) is also measured in the wind tunnel at Mach numbers 2.5 and 3.4. The drag coefficient caused by viscous friction is estimated from these wind-tunnel measurements to be 0.053, assuming that the drag caused by friction is constant in this Mach number range. Then, the drag coefficient for the clean configuration (without the step) is evaluated by the similarity rule up to Mach number 10 (Fig. 4). Adding the drag coefficient of the step, and using the blunt body value of 1 for the drag coefficient of the step, the total projectile drag is estimated by Eq. (7). The estimated variation of the drag coefficient for the projectile with the step is also indicated in Fig. 4. It is seen that the drag of the projectile with the 90-deg step is about twice the drag of the clean conical projectile. It is very possible to use a ramp of about 45 deg instead of the blunt step. There are good indications, both experimental and numerical, that such a ramp will be sufficient for initiation of combustion–detonation on the projectile. Using more optimized shapes, such as three-dimensional obstacles, for the initiation of combustion–detonation will enable reduction of the drag of the EPA projectile. Furthermore, in the EPA applications the projectile body diameter may be increased while the step or ramp height can remain about 1–2 mm. In these cases the size of the step related to the body diameter is decreased. Then the drag coefficient, in the case of the larger diameter projectiles with this small ramp, is decreased, becoming closer to the value of the drag coefficient of the clean projectile.

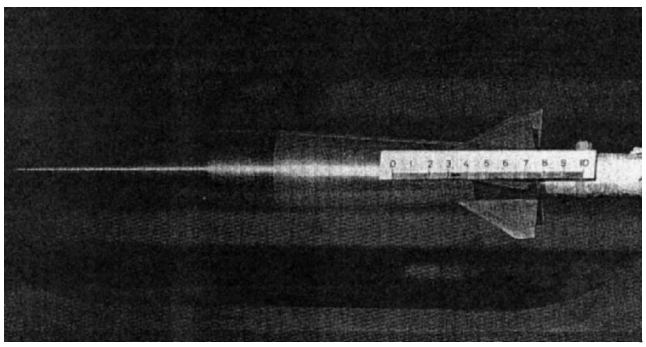

Fig. 3 EPA projectile model with a step used for wind-tunnel tests.

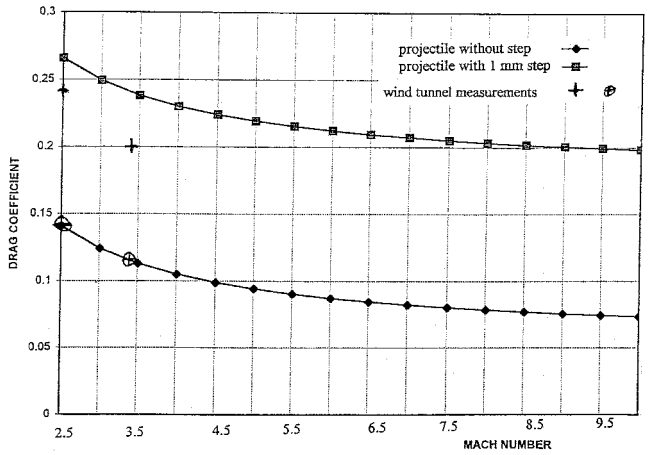

Fig. 4 Variation of the drag coefficient of the projectiles with and without the step measured in the supersonic wind tunnel as a function of the Mach number.

Calculation of the Maximum Velocity of the Projectile in the In-Tube Chemical Accelerator

The projectile is accelerated in the launching tube, increasing its velocity as it flies toward the tube exit. For a long enough tube, the projectile may reach its maximum terminal velocity $V_{\infty\,\max}$ when the thrust is balanced by the drag. In this case the acceleration is decreased to zero in Eq. (2). Therefore

$$\rho_\infty \left[\frac{\pi(\beta d)^2}{4}\right] Q\eta_P = \frac{1}{2}\rho_\infty V_{\infty\,\max}^2 \left(\frac{\pi d^2}{4}\right) C_D \tag{8}$$

The heat released in the chemical reaction of the combustible mixture Q can be related to the thermodynamic and energy characteristics of this mixture by several theoretical and empirical methods. A simple theory for the conditions across a detonation wave is presented by Fickett and Davis.[20] This simple theory is based on the assumption of a steady plane shock–detonation front in which the chemical reaction is assumed to be completed instantaneously. The reaction products ensuing behind the reaction front are assumed to be in a thermochemical equilibrium. The gas mixture is assumed to follow the ideal gas equation of state with constant specific heats. These simplifying assumptions can be acceptable as a first approximation for the conditions across a detonation front in a gaseous mixture up to moderate hypersonic speeds. The relation obtained for the heat release per unit mass in terms of the Chapman–Jouguet detonation velocity, as shown in Ref. 20,

is presented in Eq. (9). This relation was used by Lee[15] in the evaluation of the maximum projectile velocity in the RA:

$$Q = \frac{D_{CJ}^2}{2(\gamma^2 - 1)} \tag{9}$$

Substituting this value of Q into Eq. (8), the maximum velocity for the projectile is

$$\frac{V_{\infty_{max}}^2}{D_{CJ}^2} = \frac{\beta^2 \eta_p}{C_D(\gamma^2 - 1)} \tag{10}$$

Evaluation of the Combustion Region Diameter on the Projectiles in the In-Tube Accelerators

It is reasonable to assume that the thickness of the external combustion layer established over a step varies as a function of the step height and the flow Mach number. The numerical solutions of the Navier–Stokes equations with chemical reactions, which are presented in Refs. 1, 2, and 5, can be used for the preliminary estimation of the combustion-layer thickness. It was found in these calculations that the combustion-layer thickness on the 32-mm-diam projectile with a 1-mm step is estimated to be 3 step heights at Mach number 5. The combustion-layer thickness is found to increase to 5.5 step heights at Mach number 6 and to 17 step heights at Mach number 10. Thus, the combustion-layer diameter increases as the Mach number increases until combustion fills the tube. Then, β will reach its maximum value, $\beta_{max} = d_{tube}/d_{projectile}$. To utilize the thrust from this thick combustion layer the projectile must be sufficiently long. The length of the projectile must be such that the pressure field generated by the combustion–detonation ahead of the step will affect the pressure on the back of the projectile and contribute to positive thrust.

In the RA the combustion always extends from the projectile body to the tube wall. Therefore, the value of β is determined by the ratio of the tube diameter to the projectile body diameter, which is about 1.2–1.3.

Evaluation of the Acceleration of the Projectile in the In-Tube Chemical Accelerators

The acceleration of the projectile can be evaluated from the performance equation for level flight presented in Eq. (2). The thrust term in this equation can be expressed in terms of the energy of combustion and the propulsive efficiency. Equation (2) is then

$$\rho_0 \left[\frac{\pi(\beta d)^2}{4}\right] Q \eta_p - 0.5\rho_0 V_\infty^2 \left(\frac{\pi d^2}{4}\right) C_D = T - D = \frac{a}{g} W \tag{11}$$

Using the equation for the maximum velocity [Eq. (10)], the projectile acceleration evaluated by Eq. (11) can be expressed in terms of this maximum velocity by

$$\frac{a}{g} = \frac{\gamma M_\infty^2 C_D}{2} \left[\left(\frac{V_{max}}{V_\infty}\right)^2 - 1\right] \frac{p_\infty S_{projectile}}{W} \tag{12}$$

The projectile acceleration can also be expressed [using Eqs. (9) and (11)], in terms of the drag coefficient and the propulsive efficiency

$$\frac{a}{g} = \frac{M_\infty^2 C_D}{2} \left\{\left[\frac{\eta_p \beta^2}{(\gamma^2 - 1)C_D}\right] \left(\frac{M_{CJ}}{M_\infty}\right)^2 - 1\right\} \frac{p_\infty S_{projectile}}{W} \tag{13}$$

The value of the parameter $p_\infty S_{projectile}/W$ for the projectiles used in the RA tests at the University of Washington and at the U.S. Army Research Laboratory at Aberdeen, Maryland vary between 800–4000.

This analysis indicates the advantage of reducing the projectile drag to increase the performance of the projectile in the in-tube chemical accelerators. A very efficient way to reduce the projectile drag at hypersonic speeds is to utilize wave-rider configurations. A symmetrical star-shaped configuration that includes a nose section composed of 4-caret wings followed by a constant span body can be considered for a fin-stabilized operation in the RA. A star-shaped wave-rider configuration (with or without the constant span section) can be used for free flight in the EPA. The star configuration can be made aerodynamically stable, provided the c.g. is kept forward by using a heavy nose section. For the fin-guided projectiles in the RA and EPA, the edges of the constant span star-shaped body can be used as the guides, sliding on the launcher tube wall.

Comparisons Between the Analytical Evaluation and Experimental Results of Projectile Acceleration in the RA

Examination of the high-performance test results in the RA obtained at the University of Washington indicate that most

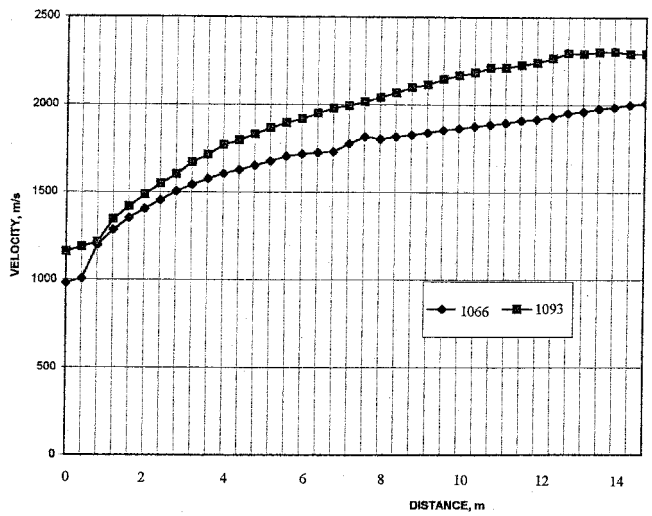

Fig. 5 Variation of the projectile velocity as a function of distance evaluated from the data of the University of Washington RA runs 1066 and 1093.

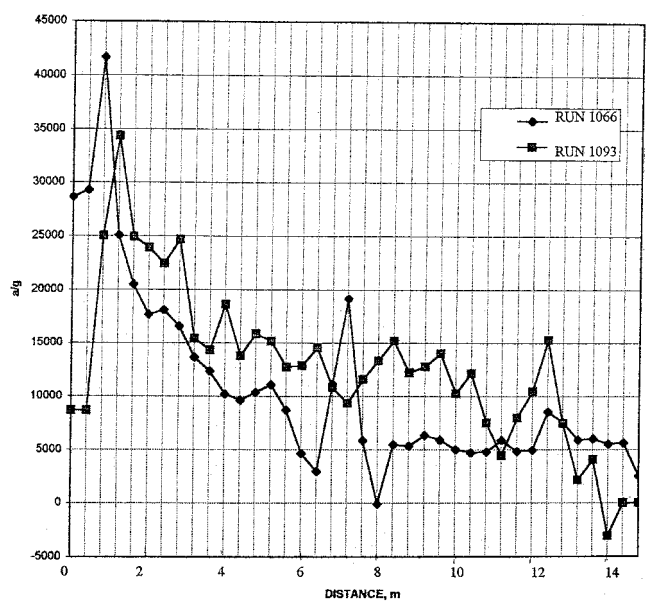

Fig. 6 Variation of the projectile acceleration as a function of distance evaluated from the data of the University of Washington RA runs 1066 and 1093.

test runs ended up in an unstart.[21,22] The unstart is defined when the projectile acceleration is terminated and the projectile disintegrates before reaching the RA tube exit. There were two test runs, using titanium-nosed projectiles, where the projectile reached a peak velocity and then remained at this peak velocity for the last 4 m of the tube. In these runs the projectile exited the accelerator tube intact. These are runs 1066 and 1093. The velocity–distance curves for these runs are presented in Fig. 5. The peak velocity of 2010 m/s for run 1066 and 2300 m/s for run 1093 is clearly observed. These peak velocities are practically constant for the last 4 m of the flight in the tube. It is therefore reasonable to define these as the maximum terminal velocities reached by the projectiles in these runs. This is also supported by the acceleration–distance curves for these runs, showing about zero acceleration at the tube exit for run 1093 (Fig. 6). For this run the initial acceleration is about 30,000 g and is reduced to about zero after 10–12 m of flight. Therefore, the measurement of the peak velocity at zero acceleration is an experimental determination of the maximum terminal velocity of the projectile as defined in Eq. (10).

Estimation of the Projectile Drag Coefficient and Propulsive Efficiency Using Experimental Time-Distance Measurements

The projectile velocity and its instantaneous acceleration measured along the tube length, shown in Figs. 5 and 6, respectively, enabled the evaluation of maximum velocity for these runs. Thus, the drag coefficient can be determined directly from the experimental data using Eq. (12), so that

$$C_D = \frac{2}{\gamma M_\infty^2} \frac{W}{p_\infty S_{\text{projectile}}} \frac{1}{(V_{\max}/V_\infty)^2 - 1} \frac{a}{g} \tag{14}$$

The variation of the drag coefficient for the projectile for runs 1066 and 1093 evaluated directly from the experimental data is presented in Fig. 7. Equation (13) is used to evaluate the propulsive efficiency

$$\eta_P = \left(\frac{\gamma^2 - 1}{\beta^2}\right)\left(C_D + \frac{1}{M_\infty^2} \frac{W}{p_\infty S_{\text{projectile}}} \frac{a}{g}\right)\left(\frac{M_\infty}{M_{\text{CJ}}}\right)^2 \tag{15}$$

The evaluated propulsive efficiency for runs 1066 and 1093 are shown in Fig. 8. The conditions for run 1066 are as follows: the mixture is $2.95CH_4 + 2O_2 + 5.7N_2$ at an initial pressure of 717 psig. The projectile is made of titanium and its weight is 109 g. It is injected at a velocity of 981 m/s, corresponding to $M = 2.7$. In the last 4 m of the tube the velocity is almost constant, slightly rising from the velocity of 2000–2010 m/s. For run 1093 the accelerator tube is divided into two sections. The first section is 2 m long and is filled with the mixture of $2.8CH_4 + 2O_2 + 5.7N_2$ at an initial pressure of 717 psig. The second section is 14 m long. It is filled with a mixture of $6CH_4 + 2O_2 + 2H_2$ at an initial pressure of 726 psig. The titanium nose projectile weight is 83.6 g. It is injected into the first stage at an initial velocity of 1161 m/s, corresponding to $M = 3.19$. The projectile velocity is increased to 1522 m/s in the first stage and at this velocity enters into the second stage. The initial Mach number at the second stage entrance is 3.39. In the last 4 m of the tube the measured projectile velocity reaches a steady maximum value of about 2300 m/s (Fig. 5).

The drag coefficient values, calculated using Eq. (14), are shown in Fig. 7. The scatter in the drag is caused by the scatter in the experimentally evaluated acceleration values obtained by the double differentiation of the x-t data. The drag coefficient for run 1093 is initially 0.2. It rises in the first stage to about 0.8 and then levels off in the first 5 m of the second stage to a value of 0.6–0.7. Then about 7 m from the entrance (5 m in the second stage) the drag coefficient starts to rise almost linearly from 0.6 to about 1.5 at about 10 m from the entrance.

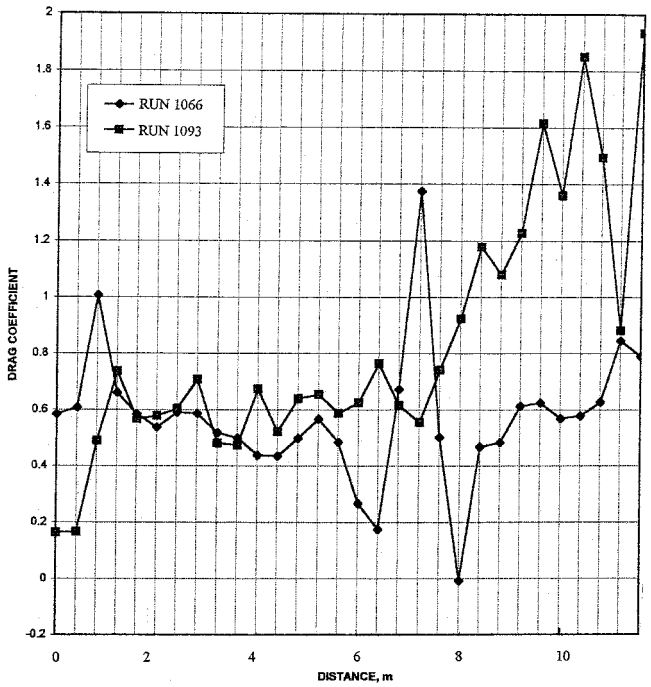

Fig. 7 Drag coefficient of the projectile calculated from the data of the University of Washington RA runs 1066 and 1093.

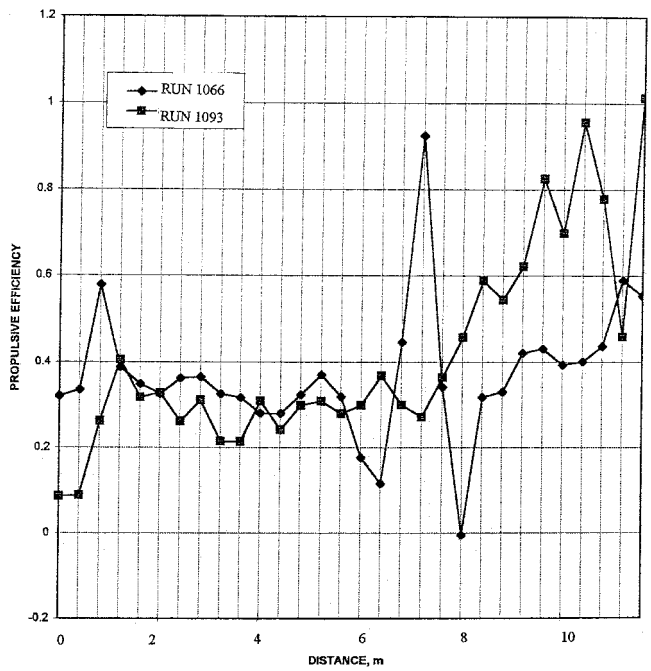

Fig. 8 Propulsive efficiency calculated from the data of the University of Washington RA runs 1066 and 1093.

These drag coefficient values are used to evaluate the propulsive efficiency using Eq. (15). The variation of the propulsive efficiency is presented in Fig. 8. The propulsive efficiency for run 1093 rises to about 0.6 in the first 2-m section. Then, in the second section the efficiency is lowered to 0.3, rising again to 0.6 at about the 8-m position and rising to 0.8 at about the 10-m position.

Thus, in the last 4–5 m of the tube in run 1093 the drag coefficient is about 1.2–1.5 and the propulsive efficiency is about 0.6–0.8. Therefore, the maximum velocity expected with these values of drag and propulsive efficiency as evalu-

ated by Eq. (10) is about 1.15–1.2 times the Chapman–Jouguet detonation velocity. The detonation velocity for the mixture in run 1066 is 1685 m/s. The maximum velocity is then $1.2 \times 1685 = 2022$ m/s. For run 1093, the detonation velocity for the mixture in the second section is 1994 m/s, so that the calculated maximum velocity for this run is 2293 m/s. These results are consistent with the analysis. They are also in agreement with the results of measurements of the limits of the maximum-attained velocity evaluated in the RA tests at the University of Washington.[21] The results of these measurements indicate that the maximum velocity obtained in all of the tests did not exceed 1.2 times the Chapman–Jouguet detonation velocity. This value of the maximum velocity is in agreement with the results presented in Refs. 15–17 and with the present analysis.

Remarks on the Unstart of Projectiles in the RA

The results of the present analysis enable better insight to the unstart phenomena experienced in many RA experiments. Unstart is caused by mechanical failure (disintegration) of the projectile during its flight in the tube. The first mode of failure may be caused by excessive mechanical and/or thermal stresses imposed on the projectile structure during the flight. This mode of mechanical failure may include also the effects of canting of the projectile toward the tube wall that may lead to the breakup of the projectile.[22] Thermal failure of the projectile can be caused by severe heat melting and even burning of the surfaces of the projectile and fins, resulting in major distortion of the projectile shape.[23] The flow over of the distorted projectile may then break it. Proper design of the projectile structure and selection of the right materials can extend the operation range of the projectile in the RA. It was found in the experiments at the University of Washington that titanium-nosed projectiles can survive the flight in their RA at least up to velocities of about Mach 6.

Another mode of unstart may be because of the development of excessive aerodynamic drag that exceeds the available thrust on the projectile. The additional drag is caused by the increased total pressure loss, for a given heat addition, as the Mach number of the accelerating projectile in the tube is increased. Because of the excessive drag the projectile decelerates, then choking may occur and the projectile flight is terminated in the unstart. This mode of unstart can also occur when the projectile is fired at a relatively low Mach number into mixtures with high heat addition.[21] For this reason the initial projectile Mach number must be above the minimum Mach number for choking for the heat addition of the mixture.

Evaluation of the Expected Performance of an Aerodynamically Stabilized Projectile in the EPA

At present there are no experiments on projectiles flying in the EPA. However, an experiment that demonstrates the flow structure with combustion on a projectile configuration similar to the proposed EPA projectile was done by Lehr.[13] This experiment was conducted at the French German Institute of Saint Louis. In a series of experiments, Lehr[13] fired projectiles of various shapes into hydrogen–air mixtures at hypersonic speeds. In one of these experiments a conical nose (15-deg half-angle cone) model with a blunt (45-deg) ramp was fired at Mach number 5 into the hydrogen–air mixture. The schlieren photograph of this run shows the details of the flowfield established because of the intersection of the detached reaction front ahead of the ramp with the nose shock wave. It is important to note that the projectile flight is straight and stable. This flowfield is in agreement with that used for the flow over the projectile in the external propulsion method. Therefore, parallel to efforts to obtain experimental data, there is justification to analyze and compute the flow over projectiles in the EPA and to estimate their performance characteristics. The energy analysis used for the calculation of the performance of projectiles in the RA is therefore applied to the aerodynamically stabilized free-flying projectile in the EPA.

In the EPA mode of operation the plan is to fire the properly shaped projectile from a powder gun or from a light gas gun into the accelerator tube filled with the premixed fuel/oxidizer mixture. The initial projectile velocity, which is higher than the detonation velocity in the mixture, is high enough to obtain combustion and generate thrust. The subcaliber projectile must be supported in the gun by a sabot as it is fired into the large diameter accelerator tube. After the projectile is separated from the sabot it flies freely in the combustible mixture in the accelerator tube, similar to the flight of a projectile in a ballistic range. The projectile is stabilized aerodynamically by relatively large fins and so its trajectory remains inside the tube and away from the tube walls. A subcaliber projectile design, which includes a small step, used for tests in the supersonic wind tunnel is shown in Fig. 3. The projectile nose is a 10-deg half-angle cone followed by a 1-mm forward-facing step. The centerbody is a 32-mm-diam short cylindrical section with a shallow 3.5-deg boattail aft section with a blunt base. This projectile weight is estimated to be 400 g. Six trapezoidal fins are added on the aftbody for aerodynamic stability of the projectile. The aerodynamic coefficients of the projectile configuration are measured in the supersonic wind tunnel. These are then used to calculate the projectile trajectory by a 6-degrees-of-freedom computer code. The calculated projectile trajectory will be used to determine the size of the fins needed to stabilize the projectile and the size of the accelerator tube. Such calculations are very important for the design of the EPA system, but in the present paper only the performance characteristics of the projectile flight are discussed.

Using the energy analysis, the acceleration of the projectile in the EPA can be evaluated by Eq. (11). For the known projectile geometry and a known mixture, the calculation of the projectile acceleration in the EPA requires the evaluation of β, η_p, and C_D. The mixture composition for EPA operation in this calculation is chosen to be $CH_4 + 2O_2 + 10CO_2$. This mixture represents a good combination of relatively high heat release, $Q/c_pT = 5.8$, a low speed of sound, $a = 284$ m/s, and a low detonation velocity, $V_{CJ} = 1201$ m/s with $\gamma = 1.302$. Using conventional gun propulsion it is possible to achieve an initial projectile velocity of about 1800 m/s, which corresponds to an initial projectile Mach number of 6.3 in this mixture.

The establishment of the combustion by the step and the extent of the combustion zone were studied by a numerical solution of the Navier–Stokes equations with chemical reactions. The results of the calculations at several hypersonic Mach numbers are presented in Refs. 1, 2, and 5. These calculations indicate that the combustion zone thickness increases almost linearly with the increase of the Mach number. It is estimated that the combustion on the 32-mm projectile will be effective in producing thrust up to a combustion diameter of 120 mm at about Mach 20. This assumption must be validated in future experiments. At present, lacking experimental measurements, this assumption seems reasonable for preliminary estimates of the EPA performance.

The drag coefficient for the projectile with the step is evaluated by Eq. (7), as discussed in a previous section. The variation of the drag coefficient for Mach number up to 10, evaluated using the wind-tunnel data, is presented in Fig. 4. It is assumed that the drag coefficient remains constant at the $M = 10$ value for higher hypersonic Mach numbers. The propulsive efficiency can be estimated from the evaluation of the thrust obtained in the CFD solutions for the EPA projectile presented in Refs. 1, 2, and 5 to be about 0.6–0.7. However, this evaluation of the propulsive efficiency is not supported by experiments at this time. Because of this uncertainty, propulsive efficiency values in the range of 0.3–0.67 are used in the preliminary evaluation of the EPA performance.

The acceleration as a function of the Mach number for initial pressure of 50 atm, assuming propulsive efficiency values of

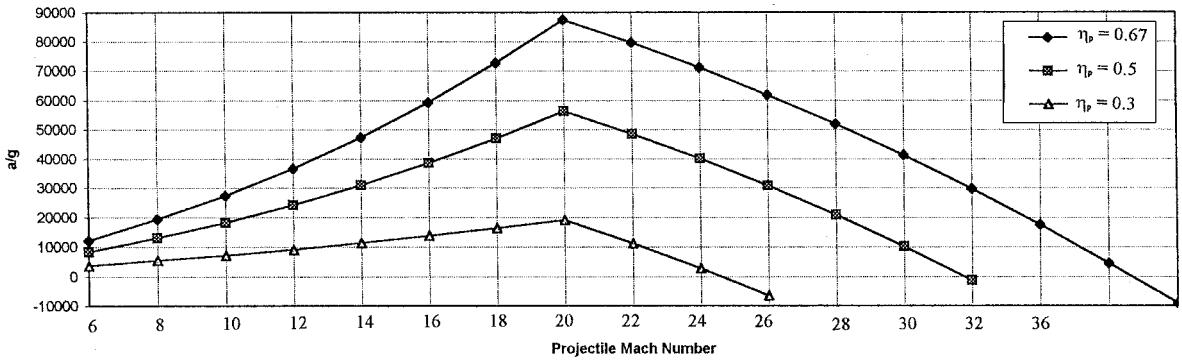

Fig. 9 Calculated variation of the projectile acceleration for the aerodynamically stabilized free-flight projectile as a function of the projectile flight Mach number in the EPA for various propulsive efficiencies.

0.67, 0.5, and 0.3, is presented in Fig. 9. The maximum acceleration is evaluated to be about 87,000 g for η_p = 0.67, 57,000 g for η_p = 0.5, and 18,000 g for η_p = 0.3, and is obtained at a flight Mach number of 20. The acceleration is then decreased as the Mach number is increasing, reaching zero at the maximum Mach numbers of 38, 32, and 25 for the propulsive efficiencies of 0.67, 0.5, and 0.3, respectively. The estimated acceleration values can be used to evaluate the length of the accelerator tube and the duration of flight. The length of the accelerator tube needed to reach Mach 34, assuming a propulsive efficiency of 0.67, is 155 m and the flight duration is about 26 ms. An accelerator length of about 300 m will be required to reach Mach 30 for a propulsive efficiency of 0.5. Considering these preliminary rough estimates, it is expected that projectile velocity in the range of 4–5 km/s can be obtained with an accelerator length of 30–80 m. As the acceleration varies linearly with the initial pressure of the mixture in the accelerator tube, higher accelerations and shorter accelerator lengths can be obtained by increasing the initial pressure of the mixture.

Summary and Conclusions

The energy balance analysis is applied to the two in-tube chemical accelerator methods: the experimentally proven RA and the proposed EPA. The acceleration of the projectile is evaluated by the balance between the chemical reaction energy and the drag work of the flying projectile.

The data from various experiments in the RA facilities at the University of Washington are used to validate the energy balance analysis. The evaluation of the performance characteristics is performed using the time–distance histories of the projectiles flight that exited intact from the RA accelerator tube. The evaluation of the drag coefficient indicates that the projectile drag coefficient increases to high values as its flight Mach number approaches the maximum attainable speed. This increase of the projectile drag coefficient is attributed to the total pressure losses leading to the choking of the supersonic flow in the narrow passage between the projectile body and the tube wall. The experimental data in the RA indicate that the drag coefficient value is about twice the propulsive efficiency value. The energy balance analysis then shows that the maximum velocity of the projectile in the RA is limited to be about 1.2 times the detonation velocity of the mixture.

The acceleration of aerodynamically stabilized free-flying projectiles in the EPA is evaluated by the energy balance analysis. At present there are no experimental results on projectile flights in the EPA. Parallel to efforts to obtain experimental data, the present paper includes a preliminary estimate of the performance characteristics of the projectile flying in the EPA. The energy analysis used for the calculation of the performance of projectiles in the RA is applied to the aerodynamically stabilized free-flying projectile in the EPA. This analysis indicates that projectile velocities of up to six times the detonation velocity can be achieved in the EPA.

The in-tube chemical accelerators, both the RA and EPA, can be scaled-up to reasonably large projectile dimensions and weights. In this case the scaling-up rules are reasonably well known because they are based on chemical combustion technology. The present analysis indicates that the RA can be used for the acceleration of projectiles to velocities of up to about 1.2 times the detonation velocity of the mixture. For mixtures with a detonation velocity up to 2.5 km/s, the corresponding maximum velocity for the projectile in the RA is about 3 km/s. It is estimated that the EPA has the potential capability to accelerate projectiles using chemical energy to hypervelocity up to six times the detonation velocity. The potential of accelerating scaled-up projectiles up to and beyond the escape velocity in the EPA suggests many possible applications. The EPA can be used as a launcher for various ground-test facilities. The capability of launching large projectiles to hypervelocity may contribute to research on penetration, impact, and other material properties. Furthermore, it was previously suggested to use the EPA as a model launcher for hypersonic free-flight ranges and for scramjet combustion test facilities. An exciting possibility is the use of a scaled-up EPA facility as the launcher of single-stage-to-orbit projectiles carrying sizable payloads. The main advantage of the proposed EPA propulsion system is that only the missile payload is fired into space. The acceleration facility and all of the fuel required for the launch are left on the ground. In such EPA facilities the launch velocity can be controlled by using various mixtures in stages along the launch tube.

Acknowledgments

Support for this research was given, in part, by the Hypersonic Research Center funded by NASA Contract NAGW3715, with I. Blankson as its Technical Monitor. D. Kruczynski from the Army Research Laboratory at Aberdeen, Maryland and A. Bruckner and C. Knowlen from the University of Washington in Seattle, Washington, were very helpful in supplying the data from their RA tests. Their help is gratefully acknowledged. It is my pleasure to acknowledge the useful discussions on the EPA technology with M. Lewis and A. K. Gupta of the University of Maryland, College Park, Maryland.

References

[1]Rom, J., Nusca, M. J., Kruczynski, D., Lewis, M., Gupta, A. K., and Sabean, J., "Recent Results with the External Propulsion Accelerator," AIAA Paper 95-2491, July 1995.

[2]Rom, J., Nusca, M. J., Kruczynski, D., Lewis, M., Gupta, A. K., and Sabean, J., "Recent Developments in the Research on the External Propulsion Accelerator," 2nd International Workshop on Ram Accelerators, Univ. of Washington, Seattle, WA, July 1995.

[3]Hertzberg, A., Bruckner, A. P., and Bogdanoff, D. W., "Ram Accelerator: A New Chemical Method for Accelerating Projectiles to Ultrahigh Velocities," *AIAA Journal*, Vol. 26, No. 2, 1988, pp. 195–203.

[4]Rom, J., "Method and Apparatus for Launching a Projectile at Hypersonic Velocity," U.S. Patent 4,932,306, June 12, 1990.

[5]Rom, J., Nusca, M. J., Kruzcynski, D., Lewis, M., Gupta, A. K., and Sabean, J., "Investigations of the Combustion Induced by a Step on a Projectile Flying at Hypersonic Speeds in the External Propulsion Accelerator," AIAA Paper 95-0259, Jan. 1995.

[6]Rom, J., Nusca, M., Lewis, M., Gupta, A. K., and Sebean, J. "Calculations of Combustion in a Scramjet Engine Model in the External Propulsion Accelerator as a Test Facility," *Proceedings of the 35th Israel Annual Conference on Aerospace Sciences* (Haifa, Israel), 1995, pp. 133–135.

[7]Rom, J., Lewis, M., Gupta, A. K., and Sebean, J., "Hypersonic Aerodynamic Test Facility Using the External Propulsion Accelerator," AIAA Paper 95-6138, April 1995.

[8]Rom, J., and Kivity, Y., "Accelerating Projectiles up to 12 km/sec. Utilizing the Continuous Detonation Propulsion Method," AIAA Paper 88-2969, July 1988.

[9]Rom, J., and Avital, G., "The External Propulsion Accelerator: Scramjet Thrust Without Interaction with the Accelerator Barrel," AIAA Paper 92-3717, July 1992.

[10]Tivanov, G., and Rom, J., "Investigation of Hypersonic Flow of a Detonable Gas Mixture Ahead of a Forward Facing Step," AIAA Paper 93-0611, Jan. 1993.

[11]Tivanov, G., and Rom, J., "Stability of Hypersonic Flow of a Detonable Gas Mixture in the Stagnation Region of a Blunt Body and a Forward Facing Step," *Proceedings of the 33rd Israel Annual Conference of Aeronautics and Astronautics* (Haifa, Israel), 1993, pp. 114–124.

[12]Tivanov, G., and Rom, J., "Stability of Hypersonic Reacting Stagnation Flow of a Detonatable Gas Mixture by Dynamical Systems Analysis," *Combustion and Flame*, Vol. 103, No. 4, 1995, pp. 311–327.

[13]Lehr, H. F., "Experiments on Shock-Induced Combustion," *Astronautica Acta*, Vol. 17, Nos. 4, 5, 1972, p. 589.

[14]Seiler, F., Patz, G., Smeets, G., and Srulijes, J., "The Rail Tube in Ram Acceleration: Feasibility Study with ISL's RAMAC 30," 2nd International Workshop on Ram Accelerators, Seattle, WA, July 1995.

[15]Lee, J. H. S., "On the Initiation of Detonation by a Hypervelocity Projectile," Zeldovich Memorial Conf. on Combustion, Voronovo, Russia, Sept. 1994.

[16]Rom, J., "Analysis of the Initiation of Detonation on a Hypervelocity Projectile and Its Maximum Velocity in the External Propulsion Accelerator," *Proceedings of the International Symposium on Shock Waves*, 1995; also TAE Rept. 729, Dec. 1994, pp. 1149–1154.

[17]Rom, J., "Analysis of the Velocity Limits of Hypervelocity Projectiles in the In-Tube Chemical Accelerators," Technion Aerospace Engineering, Rept. 756, Aug. 1995.

[18]Shevell, R. S., *Fundamentals of Flight*, 2nd ed., Prentice–Hall, Englewood Cliffs, NJ, 1989.

[19]Shapiro, A., *The Dynamics and Thermodynamics of Compressible Fluid Flows*, Vol. 1, Ronald, New York, 1953.

[20]Fickett, W., and Davis, W. C., *Detonation*, Univ. of California, Berkeley, CA, 1979.

[21]Knowlen, C., Higgins, A., and Bruckner, A., "Investigation of Operational Limits to the Ram Accelerator," AIAA Paper 94-2967, July 1994.

[22]Hinkey, J. B., Burnham, E. A., and Bruckner, A. P., "Investigation of Ram Accelerator Flow Fields Induced by Canted Projectiles," AIAA Paper 93-2186, July 1993.

[23]Naumann, K., "Thermomechanical Constraints on Ram-Accelerator Projectile Design: Limitations, Possibilities, Solutions," AIAA Paper 96-2678, July 1996.